Phase transition of interacting Bose gases in weak periodic potentials

O. Zobay and M. Rosenkranz*
Institut für Angewandte Physik, Technische Universität Darmstadt, 64289 Darmstadt, Germany
(Received 7 September 2006; published 27 November 2006)

We study the condensation of a homogeneous interacting Bose gas in the presence of a superimposed weak periodic potential. In contrast to, e.g., a harmonic trap, the periodic potential does not reduce the significance of long-wavelength fluctuations and thus influences the phase transition in a more profound way. We present general thermodynamic descriptions of the system above condensation in terms of mean-field as well as renormalization-group theory. Our approaches are based on describing the interplay between the effects of the interactions and the potential by means of a renormalization of the potential amplitude. These theories are then used to study the critical chemical potential and particle density and their dependence on the properties of the applied potential. A main result of our investigations concerns the characteristic nonperturbative momentum scale k_c of the critical interacting Bose gas. It is shown that the existence of this momentum scale becomes macroscopically manifest in the behavior of the critical thermodynamic properties.

DOI: 10.1103/PhysRevA.74.053623 PACS number(s): 03.75.Hh, 05.30.Jp, 64.60.Ak

I. INTRODUCTION

The recent realization of Bose-Einstein condensation with ultracold atoms has renewed the interest in the critical properties of interacting Bose gases [1]. Research in this area has considered systems both without and with external potentials. The particular theoretical challenge of the homogeneous system derives from the fact that the properties of the phase transition are determined by long-wavelength critical fluctuations that have to be described nonperturbatively [2–7]. In a harmonically trapped system, on the other hand, the potential effectively cuts off the influence of long-wavelength fluctuations so that critical properties, such as the critical temperature, can be calculated perturbatively with the help of the local-density approximation [8,9]. The relation between nonperturbative and perturbative physics at the phase transition was further elucidated in studies of condensation in general power-law potentials [10–12].

The present paper extends these studies of critical interacting Bose gases to the case of a homogeneous system with a superimposed weak periodic potential. We focus on the basic situation in which the potential is applied along one spatial direction only, and consider the thermodynamic limit in which the particle number and the enclosed volume tend to infinity, while the amplitude V_0 of the potential and its period λ_0 are kept fixed. The potential is supposed to be weak in the sense that V_0 remains comparable to the energy scale set by—λ_0, i.e., $V_0 \lesssim \hbar^2/m\lambda_0^2$ with m the particle mass—and the induced band gaps do not become large. We are thus considering a situation opposite to the tight-binding limit which is currently under intense study in connection with the Mott-superfluid transition [13]. In particular, the present work is not directly related to studies such as [14–16] that consider the finite-temperature phase transition in the Bose-Hubbard model.

There are several reasons for our interest in this problem. First, in contrast to the power-law and harmonic traps previously considered, a weak periodic potential does not reduce the significance of long-wavelength fluctuations for the phase transition. We can thus expect a more intricate and interesting interplay between the effects of the external potential and the critical fluctuations and a more profound influence of the potential on the phase transition. Second, for a periodic potential with a fixed period length, the local-density approximation, which forms the basis for the study of condensation in power-law and harmonic potentials [9] in the thermodynamic limit, is not applicable. The system can thus no longer be described in terms of a locally homogeneous gas, and an alternative approach has to be developed. Finally, from an experimental perspective, once the phase transition of the homogeneous gas can be examined, the study of condensation in a periodic potential will be a straightforward extension since these potentials are easily realized with the help of optical standing waves.

Our theoretical description is mainly based on a renormalization-group (RG) approach that was recently developed in connection with studies of condensation in trapped Bose gases [10,17,18]. Some of the main advantages of this approach are its flexibility, broad applicability, and ease of use, which have been demonstrated in a variety of contexts. Quantitative results have been shown to be of reasonable accuracy [18]. An important characteristic of the method is the fact that one does not have to explicitly distinguish between perturbative and nonperturbative physics and can simultaneously deal with effects occurring on different length scales, which is particularly convenient in the present context.

In the particular case of condensation in a weak periodic potential, our approach is based on describing the interplay between potential and particle interactions in terms of a renormalization of the potential amplitude. Physically, this is motivated by the fact that a weak periodic potential leads to a density modulation in the gas that is of the same shape, so that the particles still feel a sinusoidal effective potential. To introduce and illustrate this concept, we first work out the mean-field theory for the problem before turning to the full RG description. We will focus our investigations on the behavior of the critical chemical potential and particle density,

*Present address: Clarendon Laboratory, University of Oxford, Parks Road, Oxford OX1 3PU, UK.

although it would be possible to study other thermodynamic quantities as well. The study of the particle density is essentially equivalent to the investigation of the critical temperature, but somewhat simpler and more direct.

The main results of our studies can be summarized as follows. (i) It is known that the critical interacting Bose gas is characterized by a momentum scale k_c separating the regimes of perturbative and nonperturbative physics [2,7,19]. We show that the existence of this momentum scale becomes macroscopically manifest in the behavior of the critical particle density. This is because the periodic potential introduces a second independent momentum scale $2\pi/\lambda_0$ that can be used to probe k_c. (ii) We investigate in detail the effect of the renormalization of the potential amplitude on the behavior of the critical properties and show that it leads to significant quantitative consequences. In particular, in the short-wavelength limit, it is inadequate to describe the influence of the periodic potential with the help of an effective-mass model, which one would intuitively try to apply. (iii) Comparing the behavior of the critical chemical potential and the particle density, we show that only the latter reacts to the presence of a periodic potential with long wavelength. This again illustrates the fact that only the critical particle density is susceptible to long-wavelength critical fluctuations (and thus their modification by the long-wavelength potential).

The paper is organized as follows. We start by summarizing several properties of ideal Bose gases in weak periodic potentials in Sec. II. In Secs. III and IV we derive our general theoretical framework for studying the thermodynamics of the interacting Bose gas in such a potential in terms of mean-field and renormalization-group theory, respectively. In Sec. V, these methods are applied to investigate the behavior of the critical chemical potential and particle number, and we will discuss in detail the results summarized above. The paper finishes with summary and conclusions in Sec. VI.

II. IDEAL BOSE GASES IN PERIODIC POTENTIALS

In this section, we summarize some relevant material regarding ideal Bose gases in periodic potentials. We consider a system of N ideal bosons of mass m that are exposed to the potential

$$V(\mathbf{x}) = V_0 \cos(2k_l z), \tag{1}$$

which could be created, e.g., from a standing-wave laser field with wave vector k_l. In the following, we will mostly work with dimensionless variables for convenience. In particular, positions and wave vectors are written as $(q_1,q_2,q_3)=k_l(x,y,z)$ and $(\kappa_1,\kappa_2,\kappa_3)=(k_1,k_2,k_3)/k_l$, respectively. Energies are measured in units of the recoil energy $E_R=\hbar^2k_l^2/2m$, and we define the rescaled potential amplitude

$$s = \frac{V_0}{E_R}. \tag{2}$$

The system is confined to a box with (dimensionless) volume $V=L^3$ and periodic boundary conditions. The one-particle eigenfunctions are then given by

$$\psi_{\boldsymbol{\kappa}}^{(s)}(\mathbf{q}) = \frac{e^{i\kappa_1 q_1} e^{i\kappa_2 q_2}}{L} \psi_{\kappa_3}^{(s)}(q_3) \tag{3}$$

with $\kappa_j=2\pi m_j/L$ and integer m_j $(j=1,2,3)$. The functions $\psi_{\kappa_3}^{(s)}(q_3)$ are normalized solutions of the Mathieu equation

$$\left[-\frac{d^2}{dq_3^2} + s\cos(2q_3)\right]\psi_{\kappa_3}^{(s)}(q_3) = \varepsilon^{(s)}(\kappa_3)\psi_{\kappa_3}^{(s)}(q_3), \tag{4}$$

and they are indexed by the quasimomentum κ_3 in the usual way. Their eigenenergies are denoted $\varepsilon^{(s)}(\kappa_3)$. Furthermore, we introduce the energy shift

$$\Delta\varepsilon^{(s)}(\kappa_3) \equiv \varepsilon^{(s)}(\kappa_3) - \varepsilon^{(s)}(0) \tag{5}$$

relative to the ground-state energy, and we define $\varepsilon^{(s)}(\boldsymbol{\kappa})=\kappa_1^2+\kappa_2^3+\varepsilon^{(s)}(\kappa_3)$ and accordingly $\Delta\varepsilon^{(s)}(\boldsymbol{\kappa})$.

In this paper, we are interested in the case of weak potentials, i.e., small s, where, to a good degree of approximation, the eigenfunctions $\psi_{\kappa_3}^{(s)}(q_3)$ can be expanded in terms of a small number of plane waves as

$$\psi_{\kappa_3}^{(s)}(q_3) = \frac{1}{\sqrt{L}}[c_0^{(s)}(\kappa_3)e^{i\kappa_3 q_3} + c_+^{(s)}(\kappa_3)e^{i(\kappa_3+2)q_3} + c_-^{(s)}(\kappa_3)e^{i(\kappa_3-2)q_3}]. \tag{6}$$

This ansatz very accurately reproduces the exact band structure except for the omission of the third- and higher-order band gaps whose significance should be negligible for small s. Apart from a small region around $|\kappa_3|=2$, the eigenenergies following from the ansatz (6) are well approximated by

$$\varepsilon^{(s)}(\kappa_3) = \begin{cases} 1-\sqrt{(1-\kappa_3^2)^2+s^2/4}, & |\kappa_3|<1 \\ 1+\sqrt{(1-\kappa_3^2)^2+s^2/4}, & |\kappa_3|>1. \end{cases} \tag{7}$$

For $s^2 \ll (1-\kappa_3^2)^2$, this expression can be simplified to

$$\varepsilon^{(s)}(\kappa_3) = \kappa_3^2 + \frac{s^2}{8(\kappa_3^2-1)} \tag{8}$$

from which the leading-order corrections to the free-particle dispersion relation for $\kappa_3^2 \ll 1$ and $\kappa_3^2 \gg 1$ can be read off.

Up to normalization, the expansion coefficients in Eq. (6) are given by $(c_0^{(s)},c_-^{(s)},c_+^{(s)})=(1,s/\{2[e^{(s)}(\kappa_3)-\kappa_3^2]-8+8\kappa_3\},s/\{2[e^{(s)}(\kappa_3)-\kappa_3^2]-8-8\kappa_3\})$. Away from the first band gap and up to second order in s, the explicit normalized expressions read

$$c_0^{(s)}(\kappa_3) = 1 - s^2\frac{1+\kappa_3^2}{64(1-\kappa_3^2)^2}, \tag{9}$$

$$c_-^{(s)}(\kappa_3) = \frac{s}{8(\kappa_3-1)}, \quad c_+^{(s)}(\kappa_3) = -\frac{s}{8(\kappa_3+1)}. \tag{10}$$

We will study the Bose gas in the continuum limit, which is defined by letting $N,V\to\infty$ at fixed particle density $n=N/V$. The periodic potential itself is *not* modified, i.e., its amplitude and wavelength are kept constant. In the continuum limit, the one-particle density of states is given by

$$\rho(\varepsilon) = \frac{V}{(2\pi)^3}\int d^3\kappa\,\delta[\varepsilon - \varepsilon^{(s)}(\kappa)] = \frac{V}{(2\pi)^2}\kappa_3^{(s)}(\varepsilon), \quad (11)$$

where $\kappa_3^{(s)}(\varepsilon)$ denotes the inversion of $\varepsilon^{(s)}(\kappa_3)$ with $\kappa_3 \geqslant 0$. In case ε falls into a band gap, $\kappa_3^{(s)}(\varepsilon)$ is set equal to the κ_3 value of the gap. It is convenient to put

$$\kappa_3^{(s)}(\varepsilon) = \gamma^{(s)}(\varepsilon)\sqrt{\Delta\varepsilon^{(s)}} \quad (12)$$

with $\Delta\varepsilon^{(s)} \equiv \varepsilon - \varepsilon^{(s)}(0)$, so that γ directly indicates the deviation from the homogeneous potential ($s=0$) where $\gamma(\varepsilon)=1$. From Eqs. (7) and (8) it follows that $\gamma > 1 (\gamma < 1)$ for $\varepsilon < 1 (\varepsilon > 1)$, i.e., the density of states is increased compared to the homogeneous system at low energies, and decreased at high ones.

The particle number for the ideal Bose gas in the periodic potential is given by

$$N = \int d\varepsilon \frac{\rho(\varepsilon)}{\exp[x(\varepsilon - \tilde{\mu})] - 1} = \frac{V}{(2\pi)^3}\int d^3\kappa \frac{1}{\exp\{x[\varepsilon^{(s)}(\boldsymbol{\kappa}) - \tilde{\mu}]\} - 1} \quad (13)$$

with the scaled chemical potential $\tilde{\mu} = \mu / E_R$ and inverse temperature

$$x = E_R / k_B T. \quad (14)$$

The parameter x thus relates the energy scale E_R of the potential and the gas temperature T. Since condensation occurs at the critical chemical potential $\tilde{\mu}_c = \varepsilon^{(s)}(0)$, the critical particle number is determined by

$$N_c = -\frac{V}{(2\pi)^2 x}\int d\kappa_3 \ln\{1 - \exp[-x\Delta\varepsilon^{(s)}(\kappa_3)]\}. \quad (15)$$

This expression has to be evaluated numerically, in general. However, approximations can be derived for small s and the limiting cases $x \gg 1$ and $x \ll 1$ [20,21]. For $x \gg 1$, one can express the critical particle number in terms of the asymptotic series

$$(n\lambda_T^3)_c = \zeta(3/2) + \frac{s^2}{8\sqrt{\pi}}\sum_{q=0,1,\ldots}\frac{\Gamma(q+3/2)\zeta(q+3/2)}{x^q} \quad (16)$$

with the scaled thermal wavelength $\lambda_T = k_l(2\pi\hbar^2/k_B T m)^{1/2} = \sqrt{4\pi x}$, whereas for $x \ll 1$ the critical particle number is approximately given by

$$(n\lambda_T^3)_c = \zeta(3/2) - \frac{\zeta(1/2)}{8}s^2 x. \quad (17)$$

The condensation of the ideal Bose gas will be discussed further in Sec. V B (see also [20,21]).

III. MEAN-FIELD THEORY

We now turn to the investigation of the weakly interacting Bose gas and first of all consider mean-field (Hartree-Fock) theory [22]. Detailed discussions regarding the applicability of mean-field (MF) theory to the study of critical homogeneous and trapped Bose gases can be found, e.g., in [9,12,19,23,24]. For the homogeneous gas, MF theory fails to account for the shift in the critical temperature since it does not properly describe the influence of long-wavelength critical fluctuations. Since these fluctuations are also relevant in the periodic potential, we can expect a similar failure in the present case. Nevertheless, the study of MF theory is still useful, as we will see, since it provides some useful qualitative physical insights and helps to set the stage for the subsequent RG calculation. Furthermore, it allows us to determine the critical chemical potential to leading order in the scattering length, thus providing a point of comparison for the RG results.

Within MF theory, the number density above the critical point is given by

$$n(\mathbf{q}) = \frac{V}{(2\pi)^3}\int d^3\kappa \frac{|\phi_\kappa^{(s)}(\mathbf{q})|^2}{\exp\{x[\varepsilon_{\mathrm{MF}}^{(s)}(\boldsymbol{\kappa}) - \tilde{\mu}]\} - 1}. \quad (18)$$

The single-particle wave functions $\phi_{\boldsymbol{\kappa}}^{(s)}(\mathbf{q})$ are determined by

$$[-\nabla^2 + s\cos(2q_3)]\phi_{\boldsymbol{\kappa}}^{(s)}(\mathbf{q}) + 2\nu(\mathbf{q})\phi_{\boldsymbol{\kappa}}^{(s)}(\mathbf{q}) = \varepsilon_{\mathrm{MF}}^{(s)}(\boldsymbol{\kappa})\phi_{\boldsymbol{\kappa}}^{(s)}(\mathbf{q}). \quad (19)$$

To obtain this relation, we have used the fact that for an (unscaled) s-wave contact potential $V(\mathbf{x}-\mathbf{x}') = u_0\delta(\mathbf{x}-\mathbf{x}')$ with the coupling constant $u_0 = 4\pi\hbar^2 a/m$ and the scattering length a, the Hartree-Fock self-energy is given by $\hbar\Sigma^*(\mathbf{x},\mathbf{x}') = 2u_0 n(\mathbf{x})\delta(\mathbf{x}-\mathbf{x}')$. The quantity ν appearing in Eq. (19) is defined by $\nu = u_0 n / E_R$, when expressed in terms of unscaled variables. With scaled quantities, $\nu(\mathbf{q}) = 16\pi^{3/2}\hat{a}\sqrt{x}n(\mathbf{q})$ where the scattering length is given as $\hat{a} = (ak_l)/\lambda_T$.

Equations (18) and (19) have to be solved self-consistently. To this end, we assume that, for a weak periodic potential, the functions $\phi_{\boldsymbol{\kappa}}^{(s)}(\mathbf{q})$ can be expanded as

$$\phi_{\boldsymbol{\kappa}}^{(s)}(\mathbf{q}) = \frac{1}{\sqrt{V}}e^{i\kappa_1 q_1}e^{i\kappa_2 q_2}[d_0^{(s)}(\kappa_3)e^{i\kappa_3 q_3} + d_+^{(s)}(\kappa_3)e^{i(\kappa_3+2)q_3} + d_-^{(s)}(\kappa_3)e^{i(\kappa_3-2)q_3}] \quad (20)$$

corresponding to the case of the ideal gas in Sec. II. Similar expansions were used in the context of zero-temperature Bose-Einstein condensates in periodic potentials, e.g., in Refs. [26,27]. With this ansatz, we can approximate the number density as

$$n(\mathbf{q}) = \frac{1}{(2\pi)^3}\int d^3\kappa \frac{1}{\exp\{x[\varepsilon_{\mathrm{MF}}^{(s)}(\boldsymbol{\kappa}) - \tilde{\mu}]\} - 1} + \cos(2q_3) \times \frac{2}{(2\pi)^3}\int d^3\kappa \frac{d_0^{(s)}(\kappa_3)[d_+^{(s)}(\kappa_3) + d_-^{(s)}(\kappa_3)]}{\exp\{x[\varepsilon_{\mathrm{MF}}^{(s)}(\boldsymbol{\kappa}) - \tilde{\mu}]\} - 1} \equiv n_0 + \Delta n\cos(2q_3) \quad (21)$$

with $n_0 = N/V$ the *average* particle density and Δn the amplitude of the density modulation. In obtaining Eq. (21) we use that $|d_0|^2 + |d_+|^2 + |d_-|^2 = 1$ because of normalization (this yields the term n_0). Furthermore, we neglect terms containing the product $d_+ d_-$ since they only yield a small

contribution compared to the terms with $d_0(d_+ + d_-)$. Inserting Eq. (21) into Eq. (19), we obtain

$$[-\nabla^2 + (s + 2\Delta\nu)\cos(2q_3)]\phi_{\boldsymbol{\kappa}}^{(s)}(q) + 2\nu_0\phi_{\boldsymbol{\kappa}}^{(s)}(\mathbf{q}) = \varepsilon_{\mathrm{MF}}^{(s)}(\boldsymbol{\kappa})\phi_{\boldsymbol{\kappa}}^{(s)}(\mathbf{q}) \tag{22}$$

with $\nu_0 = u_0 n_0 / E_R = 16\pi^{3/2}\hat{a}\sqrt{x}n_0$ and accordingly for $\Delta\nu$. From this equation we recognize that, within the mean-field picture, the individual particles experience an effective potential $V_{\mathrm{eff}}(\mathbf{q}) = V(\mathbf{q}) + 2\Delta\nu\cos(2q_3)$, which is still sinusoidal [on the basis of the approximations leading to Eq. (21)]. This means, first of all, that Eq. (22) can be discussed with the help of the results for the single-particle Mathieu equation of Sec. II. We see that the particle interactions modify the amplitude of the effective potential to $s_{\mathrm{eff}} = s + 2\Delta\nu$. Using Eqs. (9) and (10), one concludes that for positive s and low enough temperatures, i.e., large $x = E_R/k_BT$, Δn and $\Delta\nu$ will be negative. This means that for repulsive interactions ($u_0 > 0$) the amplitude of V_{eff} is lowered as compared to the bare $V(\mathbf{q})$. Physically, this is due to the fact that for $|\kappa_3| < 1$ the eigenfunctions $\psi_{\kappa_3}^{(s)}(q_3)$ of Eq. (4) have their density maxima at the positions of the minima of $V(\mathbf{q})$ so that the external and the mean-field potentials are out of phase. Qualitatively similar conclusions for a Bose-Einstein condensate at $T = 0$ and its effective potential were derived in [28]. For $|\kappa_3| > 1$, however, the density maxima coincide with the *maxima* of $V(x)$. For larger temperatures (i.e., smaller x) this simple argument therefore no longer applies, but numerical calculations show that s_{eff} keeps decreasing for decreasing x within the mean-field approach (with RG, s_{eff} goes through a minimum at very small x).

The eigenenergy $\varepsilon_{\mathrm{MF}}^{(s)}(\boldsymbol{\kappa})$ of Eq. (22) is given by

$$\varepsilon_{\mathrm{MF}}^{(s)}(\boldsymbol{\kappa}) = \varepsilon^{(s_{\mathrm{eff}})}(\boldsymbol{\kappa}) + 2\nu_0 \tag{23}$$

with $\varepsilon^{(s_{\mathrm{eff}})}(\boldsymbol{\kappa})$ the single-particle energy for the ideal gas with potential amplitude s_{eff}. We also see that $\varepsilon_{\mathrm{MF}}^{(s)}(\boldsymbol{\kappa})$ is shifted by the average mean-field energy $2\nu_0$ compared to the noninteracting case, just as for the homogeneous Bose gas. Furthermore, the amplitudes $d_{0,\pm}^{(s)}$ of Eq. (20) are given by the Mathieu coefficients $c_{0,\pm}^{(s_{\mathrm{eff}})}$ discussed in Sec. II.

Using Eq. (23), we can write

$$\nu_0 = \nu_0(s_{\mathrm{eff}}) = \frac{2\hat{a}\sqrt{x}}{\pi^{3/2}} \int d^3\kappa \frac{1}{\exp\{x[\varepsilon^{(s_{\mathrm{eff}})}(\boldsymbol{\kappa}) + 2\nu_0(s_{\mathrm{eff}}) - \tilde{\mu}]\} - 1}, \tag{24}$$

$$\Delta\nu = \Delta\nu(s_{\mathrm{eff}}) = \frac{4\hat{a}\sqrt{x}}{\pi^{3/2}} \int d^3\kappa \frac{c_0^{(s_{\mathrm{eff}})}(\kappa_3)[c_+^{(s_{\mathrm{eff}})}(\kappa_3) + c_-^{(s_{\mathrm{eff}})}(\kappa_3)]}{\exp\{x[\varepsilon^{(s_{\mathrm{eff}})}(\boldsymbol{\kappa}) + 2\nu_0(s_{\mathrm{eff}}) - \tilde{\mu}]\} - 1}. \tag{25}$$

The self-consistent solution of Eqs. (21) and (22) is now equivalent to determining s_{eff} from the condition

$$s_{\mathrm{eff}} = s + 2\Delta\nu(s_{\mathrm{eff}}). \tag{26}$$

This condition expresses quantitatively that the renormalized amplitude s_{eff} is given by $s + 2\Delta\nu$, but $\Delta\nu$ in turn depends on s_{eff}. In general, the solution of Eq. (26) is quite complicated since one has to determine ν_0 from the implicit equation (24). However, we are interested in the phase transition point, which is determined by

$$\tilde{\mu}_c = \varepsilon^{(s_{\mathrm{eff}})}(\boldsymbol{\kappa} = \mathbf{0}) + 2\nu_0(s_{\mathrm{eff}}). \tag{27}$$

In this case, Eqs. (24) and (25) simplify to

$$\nu_0(s_{\mathrm{eff}}) = \frac{2\hat{a}\sqrt{x}}{\pi^{3/2}} \int d^3\kappa \frac{1}{\exp[x\Delta\varepsilon^{(s_{\mathrm{eff}})}(\boldsymbol{\kappa})] - 1}, \tag{28}$$

$$\Delta\nu(s_{\mathrm{eff}}) = \frac{4\hat{a}\sqrt{x}}{\pi^{3/2}} \int d^3\kappa \frac{c_0^{(s_{\mathrm{eff}})}(\kappa_3)[c_+^{(s_{\mathrm{eff}})}(\kappa_3) + c_-^{(s_{\mathrm{eff}})}(\kappa_3)]}{\exp[x\Delta\varepsilon^{(s_{\mathrm{eff}})}(\boldsymbol{\kappa})] - 1} \tag{29}$$

with $\Delta\varepsilon^{(s_{\mathrm{eff}})}(\boldsymbol{\kappa}) = \varepsilon^{(s_{\mathrm{eff}})}(\boldsymbol{\kappa}) - \varepsilon^{(s_{\mathrm{eff}})}(\mathbf{0})$. Equations (28) and (29) are easily evaluated numerically, so that the condition (26) is readily solved for s_{eff}, e.g., by iteration. In this way, all mean-field critical quantities can be calculated. To facilitate the comparison to the subsequent RG calculation, we note that Eq. (29) can be written as

$$\Delta\nu(s_{\mathrm{eff}}) = \frac{8\hat{a}\sqrt{x}}{\sqrt{\pi}} \int_0^\infty d\varepsilon \frac{\mathcal{F}_1^{(s_{\mathrm{eff}})}[\varepsilon + \varepsilon^{(s_{\mathrm{eff}})}(0)]}{\exp(x\varepsilon) - 1}, \tag{30}$$

where the function $\mathcal{F}_1$ is defined by

$$\mathcal{F}_1^{(s)}(\varepsilon) = \int_0^{\kappa_3^{(s)}(\varepsilon)} d\kappa_3 c_0^{(s)}(\kappa_3)[c_+^{(s)}(\kappa_3) + c_-^{(s)}(\kappa_3)] \tag{31}$$

with $\kappa_3^{(s)}(\varepsilon)$ determined as discussed below Eq. (11).

Before discussing the physical content of this mean-field approach, it is convenient to first introduce the RG description of the system.

IV. RENORMALIZATION-GROUP THEORY

Mean-field theory does not properly account for the influence of long-wavelength critical fluctuations on the phase transition. In general, it therefore cannot be used to determine the critical particle number and temperature. A possibility to go beyond MF theory and to overcome these difficulties is offered by the momentum-shell RG method [29]. Since the 1970s, a number of papers have used this approach in connection with studies of weakly interacting boson systems (see, e.g., [30–35]). While some of these works were mainly concerned with the calculation of critical exponents [30,31,34], others used the RG flow equations to investigate critical thermodynamic properties. In Ref. [32], the critical temperature of the 2D Bose gas was examined, whereas [33,35] studied the 3D gas using RG equations for the *condensed* phase. These equations, however, do not yield the correct behavior for, e.g., the critical temperature [24]. After clarifying the relation between the flow equations for the condensed and the uncondensed phase [25], an RG approach

for the uncondensed phase was developed and successfully used to investigate the critical thermodynamic properties of homogeneous, trapped, and disordered Bose gases [10,17,18]. In this section, we will outline how these methods are adapted to the case of a weak external periodic potential and derive the corresponding flow equations.

The partition function of the interacting Bose gas can be represented in terms of a functional integral

$$Z = \int \mathcal{D}\phi^* \int \mathcal{D}\phi e^{-S[\phi,\phi^*]} \tag{32}$$

with the Euclidean action

$$S[\phi,\phi^*] = \int_0^x d\tau \int d^3\mathbf{q} \left\{ \phi^*(\tau,\mathbf{q}) \left[\frac{\partial}{\partial\tau} - \nabla^2 + V(\mathbf{q}) - \tilde{\mu} \right] \phi(\tau,\mathbf{q}) + \frac{g}{2}|\phi(\tau,\mathbf{q})|^4 \right\}. \tag{33}$$

The complex-valued bosonic fields $\phi(\tau,\mathbf{q})$ are periodic in the imaginary time τ and obey spatial periodic boundary conditions. They can be expanded as

$$\phi(\tau,\mathbf{q}) = \sum_{n,\mathbf{k}} a_{n,\mathbf{k}} e^{-i\omega_n\tau} \psi_{\boldsymbol{\kappa}}^{(s)}(\mathbf{q}) \tag{34}$$

with $\psi_{\boldsymbol{\kappa}}^{(s)}(\mathbf{q})$ representing single-particle eigenfunctions of the periodic potential as defined by Eq. (3) and $\omega_n = 2\pi n/x$ denoting the Matsubara frequencies. The sum in Eq. (34) only includes spatial eigenfunctions with energies below a cutoff energy $\varepsilon_\Lambda = \Lambda^2 + \varepsilon^{(s)}(0)$, with Λ denoting the corresponding cutoff momentum.

The overall strategy for the application of our RG approach is as follows. As in Sec. III, the system is considered to be above the critical point. The bosonic fields are split into a slow and a fast-field component, i.e., $\phi(\tau,\mathbf{q}) = \phi_<(\tau,\mathbf{q}) + \phi_>(\tau,\mathbf{q})$, where the fast-field component $\phi_>$ only contains spatial eigenfunctions with energies within an infinitesimally small shell near the cutoff. After expanding the Euclidean action S up to second order in $\phi_>$, the fast field is eliminated through a Gaussian integration and the result is expanded up to second order in the coupling strength. Applying the lowest-order derivative expansion, the functional integral can again be written in the form (32) and (33), where the integration is now over the slow field $\phi_<$ only. As a consequence of integrating out the fast field, the parameters in the Euclidean action receive infinitesimal corrections. In contrast to the case of the power-law trap, however, it is now not only the chemical potential $\tilde{\mu}$ and the coupling constant g that become renormalized, but also the external potential through the modification of the amplitude s, as one would already expect from the mean-field approach. To calculate the partition function, the process of eliminating thin shells is repeated until the fields ϕ have been integrated out completely. Details of the calculation for a homogeneous Bose gas and for external power-law potentials are given in [10,17,18,36]. References [17,36] also provide a discussion of the general approximations involved in this kind of RG calculation, such as the polynomial expansion of the effective action, the derivative expansion, and the role of the cutoff. Further approximations specific to the periodic potential are discussed below.

Following the general approach described above, we will now outline some details of the derivation and work out the modifications and extensions to the previous calculations of Refs. [10,17,18,36]. First of all, we describe how to determine the thin shells of eigenfunctions to be integrated out in each step. Since the eigenfunctions can be indexed by their wave vector $\boldsymbol{\kappa}$, this is equivalent to defining corresponding volumes in $\boldsymbol{\kappa}$ space. We will associate a running parameter l with the elimination of the energy shells where l changes from 0 to ∞ in the course of the integration and increases by dl at each step. We now recall that for the homogeneous Bose gas, we integrate out a spherical momentum shell of radius Λe^{-l} and width $\Lambda e^{-l} dl$ in each step with Λ the initial cutoff momentum (note that here we disregard the trivial rescaling that would restore all momenta to their initial values after each step). In other words, in a step going from $l_0 = l$ to $l_1 = l + dl$ we integrate out all states in $\boldsymbol{\kappa}$ space between the surfaces determined by

$$\kappa_1^2 + \kappa_2^2 + \kappa_3^2 = \Lambda^2 e^{-2l_0}$$

and

$$\kappa_1^2 + \kappa_2^2 + \kappa_3^2 = \Lambda^2 e^{-2l_1}.$$

We now take the periodic potential into account and first of all assume that the potential amplitude s remains *unchanged*. The obvious generalization of the prescription for the homogeneous gas is then to integrate over all states between the surfaces

$$\kappa_1^2 + \kappa_2^2 + \varepsilon^{(s_0)}(\kappa_3) = \Lambda^2 e^{-2l_0} + \varepsilon^{(s_0)}(0) \tag{35}$$

and

$$\kappa_1^2 + \kappa_2^2 + \varepsilon^{(s_1)}(\kappa_3) = \Lambda^2 e^{-2l_1} + \varepsilon^{(s_1)}(0) \tag{36}$$

with $s_0 = s_1 = s$. In particular, we see that the cross section that is obtained by intersecting the volume defined by Eqs. (35) and (36) with the plane $\kappa_3 = 0$ coincides with the one for the homogeneous gas. The new shells thus start to get somewhat deformed when we move away from the plane $\kappa_3 = 0$, the deformation being determined by the behavior of $\varepsilon^{(s)}(\kappa_3)$.

In the full problem, the amplitude s becomes a function of l, and we take this into account by setting $s_0 = s(l_0)$ and $s_1 = s(l_1)$ in the above equations (35) and (36). The number of eigenstates $d(l)dl$ within an energy shell thus obtains a contribution due to the variation of $s(l)$. Explicitly, the density $d(l)$ is found to be given by

$$d(l) = \frac{V\Lambda^3}{2\pi^2} \xi(l) e^{-3l}, \tag{37}$$

where

$$\xi(l) = \gamma^{(s)} + \frac{1}{2}\frac{ds}{dl}\left(\frac{2x}{b(l)}\right)^{3/2} \int_0^{\kappa_3^{(s)}} d\kappa_3 \frac{\partial \Delta\varepsilon^{(s)}(\kappa_3)}{\partial s}. \tag{38}$$

In Eq. (38), we have set $s = s(l)$; $\gamma^{(s)}$ and $\kappa_3^{(s)}$ are evaluated at the current cutoff energy

$$\varepsilon_\Lambda(l) = \Lambda^2 e^{-2l} + \varepsilon^{(s)}(0) \tag{39}$$

[see Eq. (12)]; and $b(l)=xe^{-2l}/x_\Lambda$ with $x_\Lambda=E_R\beta_\Lambda=E_Rm/\hbar^2(\Lambda k_l)^2$. The first term in Eq. (38) can be obtained directly from Eq. (11) [set $d(l)dl=\rho(\varepsilon)d\varepsilon$]. It thus gives the contribution to the density of states arising from the periodic potential disregarding the change in $s(l)$. This change is accounted for by the second term in Eq. (38), which is proportional to ds/dl. However, the numerical calculations show that this term typically bears only a small effect on the thermodynamic results.

Having defined the energy shells, we can now discuss in more detail the effective action $S_{\text{eff}}[\phi_<,\phi_<^*]$ resulting from the elimination of the fast field $\phi_>(\tau,\mathbf{q})$. As derived, e.g., in Ref. [10], S_{eff} can be approximated as

$$S_{\text{eff}}[\phi_<,\phi_<^*] \approx S[\phi_<,\phi_<^*] + \frac{1}{2}\text{Tr}[\ln(\hat{G}_0^>)^{-1}] - \frac{1}{2}\text{Tr}(\hat{G}_0^>\hat{\Sigma}) - \frac{1}{4}\text{Tr}[(\hat{G}_0^>\hat{\Sigma})^2] \tag{40}$$

with $\hat{G}_0^>$ the bare Green's function for the high-energy field and $\hat{\Sigma}$ the self-energy for the low-energy field [36]. The "Tr" symbol denotes the trace in both the functional and the internal space of the operators. For the trace involving only $(\hat{G}_0^>)^{-1}$, one obtains

$$\frac{1}{2}\text{Tr}[\ln(\hat{G}_0^>)^{-1}] = -\sum_{\substack{\varepsilon_\Lambda(l+dl) \\ \leqslant\varepsilon^{(s)}(\boldsymbol{\kappa})\leqslant\varepsilon_\Lambda(l)}} \ln\{1-e^{-x[\varepsilon_\Lambda(l)-\tilde{\mu}(l)]}\}. \tag{41}$$

The sum appearing in Eq. (41) represents the summation over all the states in the energy shell defined above. The other two traces of Eq. (40) are evaluated as

$$\text{Tr}[\hat{G}_0^>\hat{\Sigma}] = 4gN_{\text{BE}}(l)\int_0^x d\tau\int d^3\mathbf{q}|\phi_<(\tau,\mathbf{q})|^2 A[\varepsilon_\Lambda(l),\mathbf{q}] \tag{42}$$

and

$$\text{Tr}[\hat{G}_0^>\hat{\Sigma}\hat{G}_0^>\hat{\Sigma}] = 2g^2\left\{4xN_{\text{BE}}(l)[1+N_{\text{BE}}(l)] + \frac{1+2N_{\text{BE}}(l)}{2[\varepsilon_\Lambda(l)-\tilde{\mu}]}\right\} \times \int_0^x d\tau\int d^3\mathbf{q}|\phi_<(\tau,\mathbf{q})|^4 A[\varepsilon_\Lambda(l),\mathbf{q}] \tag{43}$$

with $N_{\text{BE}}(l)=(\exp\{x[\varepsilon_\Lambda(l)-\tilde{\mu}]\}-1)^{-1}$ the Bose-Einstein distribution at the current cutoff energy. The function

$$A[\varepsilon_\Lambda(l),\mathbf{q}] = \sum_{\substack{\varepsilon_\Lambda(l+dl) \\ \leqslant\varepsilon^{(s)}(\boldsymbol{\kappa})\leqslant\varepsilon_\Lambda(l)}} |\psi_{\boldsymbol{\kappa}}^{(s)}(\mathbf{q})|^2 \tag{44}$$

contains a summation over the squared moduli of all one-particle eigenfunctions within the energy shell at point $\mathbf{q}$. Using the expansion (6) for the eigenfunctions $\psi_{\kappa_3}^{(s)}(q_3)$ and applying similar arguments regarding the coefficients c_i as in the derivation of Eq. (21), one can show that the function $A[\varepsilon_\Lambda(l),\mathbf{q}]$ can be approximated as

$$A[\varepsilon_\Lambda(l),\mathbf{q}] = \frac{\Lambda^3}{2\pi^2}[\xi(l)+\eta(l)\cos(2q_3)]e^{-3l}dl \tag{45}$$

with $\xi(l)$ given by Eq. (38) and

$$\eta(l) = \sqrt{\frac{2x}{b(l)}}\mathcal{F}_1^{(s)}(l) + \frac{1}{2}\frac{ds}{dl}\left(\frac{2x}{b(l)}\right)^{3/2}\mathcal{F}_2^{(s)}(l), \tag{46}$$

where $\mathcal{F}_1^{(s)}(l)$ is defined by Eqs. (31) and (39), and

$$\mathcal{F}_2^{(s)}(l) = \int_0^{\kappa_3^{(s)}} d\kappa_3 \frac{\partial\Delta\varepsilon^{(s)}(\kappa_3)}{\partial s} c_0^{(s)}(\kappa_3)[c_+^{(s)}(\kappa_3)+c_-^{(s)}(\kappa_3)]. \tag{47}$$

Inserting the two pieces of Eq. (45) into Eq. (42), we see that the term containing $\xi(l)$ can be considered an infinitesimal correction to μ in the effective action S_{eff} of Eq. (40), similar to the case of the homogeneous Bose gas and the power-law trap. The term containing $\eta(l)$, however, gives rise to a modification in the amplitude of the periodic potential due to the appearance of the factor $\cos(2q_3)$. Such a direct renormalization of the potential was absent in the case of the power-law trap. From the insertion of Eq. (45) into the second-order trace (43), we keep only the term containing $\xi(l)$, which yields a correction to the coupling constant g. The term with $\eta(l)$, which has no counterpart in the original action S, is neglected since it is of higher order in the small quantities g and s than the other renormalizations and can thus be expected to be of lesser significance.

Following these arguments, one can readily derive the flow equations for μ, g, and s. To be consistent with the work of [10,17,18,36], we write them in terms of the dimensionless quantities $M(l)=x_\Lambda\tilde{\mu}(l)e^{2l}$ and $\tilde{G}(l)=x_\Lambda^2\Lambda^3 g(l)e^l/x$. These definitions also take the trivial rescaling into account, which we have not considered explicitly so far. The flow equations then read

$$\frac{dM(l)}{dl} = 2M(l) - 2\frac{\xi(l)}{2\pi^2}\tilde{G}(l)b(l)N_{\text{BE}}(l), \tag{48}$$

$$\frac{d\tilde{G}(l)}{dl} = \tilde{G}(l) - \tilde{G}(l)^2\frac{\xi(l)}{2\pi^2}b(l)\left\{4b(l)N_{\text{BE}}(l)[1+N_{\text{BE}}(l)] + \frac{N_{\text{BE}}(l)}{E_>(l)-M(l)}\right\}, \tag{49}$$

$$\frac{ds}{dl} = -\frac{\frac{2}{\pi^2}\sqrt{\frac{b(l)}{2x}}\mathcal{F}_1(l)\tilde{G}(l)b(l)N_{\text{BE}}(l)}{1+\frac{1}{\pi^2}\sqrt{\frac{2x}{b(l)}}\mathcal{F}_2(l)\tilde{G}(l)b(l)N_{\text{BE}}(l)} \tag{50}$$

with the Bose-Einstein distribution $N_{\text{BE}}(l)=1/(\exp\{b(l)\times[E_>(l)-M(l)]\}-1)$ and the rescaled cutoff energy $E_>(l)=\varepsilon_\Lambda(l)e^{2l}=1/2+x\varepsilon^{(s(l))}(0)/b(l)$. Note that to derive Eq. (49), we have also replaced the term $[1+2N_{\text{BE}}(l)]/2[\varepsilon_\Lambda(l)$

$-\tilde{\mu}]$ of Eq. (43) by $N_{\mathrm{BE}}(l)/[\varepsilon_\Lambda(l)-\tilde{\mu}]$ for simplicity. This amounts to neglecting the short-distance renormalization of $\tilde{G}$ due to two-body interactions [18,33]. The physical scattering length is then related to the initial conditions for the integration of the flow equations via $\hat{a}=\tilde{G}(0)\sqrt{2\pi b(0)}/8\pi^2$.

Using Eq. (41), the scaled free energy of the system is calculated as

$$W=-\frac{x_\Lambda}{x}\ln Z=\frac{V\Lambda^3}{2\pi^2 b(0)}\int_0^\infty dl e^{-3l}\xi(l)\ln\{1-e^{-b(l)[E_>(l)-M(l)]}\}$$
$$\equiv\frac{V\Lambda^3}{2\pi^2 b(0)}\mathcal{I}[M(0),\tilde{G}(0),b(0);s(0),x] \qquad (51)$$

with $\mathcal{I}$ representing the integral of the first line of Eq. (51), which depends on the initial conditions $M(0),\tilde{G}(0),b(0)$ for the integration of the flow equations as well as the parameters $s(0)$ and x of the periodic potential. From Eq. (51), the particle number is obtained through $N=-\partial W/\partial M(0)$.

The critical trajectories that represent the system at the phase transition are characterized by the unrescaled chemical potential $\tilde{\mu}(l)=M(l)e^{-2l}/x_\Lambda$ asymptotically reaching the bottom $\varepsilon^{(s(l))}(0)$ of the renormalized external potential, i.e., $\lim_{l\to\infty}[\tilde{\mu}(l)-\varepsilon^{(s(l))}(0)]=0$. From a critical trajectory with initial conditions $\{M^{(\mathrm{cr})}(0),\tilde{G}^{(\mathrm{cr})}(0),b^{(\mathrm{cr})}(0);s(0)\}$ the critical particle density is then obtained as

$$(n\lambda_T^3)_c\equiv f_c=-\sqrt{\frac{2}{\pi}b(0)}$$
$$\times\frac{\partial}{\partial M(0)}\mathcal{I}[M^{(\mathrm{cr})}(0),\tilde{G}^{(\mathrm{cr})}(0),b^{(\mathrm{cr})}(0);s(0),x]. \qquad (52)$$

Numerically, the derivative can be evaluated efficiently using the methods described in Ref. [17]. From the knowledge of the critical density f_c at fixed temperature, it is straightforward to calculate, e.g., the interaction-induced shift in the critical temperature relative to the ideal gas at fixed density, but in the following we will focus on the behavior of the critical density for simplicity.

It is worthwhile to comment on a few properties of the flow equations (48)–(51). (i) In the case of power-law potentials, the flow equations for M and $\tilde{G}$ do not explicitly depend on the density of states in the trap, but are identical to the ones for the homogeneous Bose gas [10]. The properties of the trap enter only through the equation for W. Such a behavior is in agreement with the local-density approximation (LDA) in which the trapped gas is regarded as locally homogeneous at each point. For the periodic potentials considered here, however, the LDA is not applicable and we find the density of states to explicitly enter the equations for M and $\tilde{G}$ through the function $\xi(l)$. A similar behavior was also observed for the case of a confining square-well potential in Ref. [35]. (ii) In contrast to previous studies, the instantaneous cutoff energy $E_>(l)=1/2+x\varepsilon^{(s(l))}(0)/b(l)$ acquires nontrivial behavior through its dependence on the varying potential amplitude $s(l)$. This dependence will be seen to crucially influence the critical thermodynamic properties. (iii) The renormalization of the potential is determined by Eq. (50). For small changes Δs we can easily relate this expression to the mean-field theory of Sec. III. Under this condition, we find $\Delta s=s_{\mathrm{eff}}-s\approx 2\Delta\nu(s)$ in the MF calculation. In the RG approach, we have $\Delta s=\int_0^\infty dl\, ds(l)/dl$. The denominator in Eq. (50) is only of minor significance and may be neglected, in general. Furthermore, we may approximately set $\tilde{G}(l)=8\pi^2\hat{a}/\sqrt{2\pi b(l)}$ in Eq. (50) [18]. After a suitable variable substitution, one can readily show that the RG result from Eq. (50) essentially coincides with Eq. (30). This conclusion is confirmed by the numerical calculations.

V. CRITICAL PROPERTIES

In this section, we will use the theoretical methods introduced above to study the thermodynamic properties of an interacting Bose gas in a weak periodic potential at the phase transition. In particular, we will consider the critical chemical potential $(\beta\mu)_c\equiv(x\tilde{\mu})_c$ and particle density $f_c=(n\lambda_T^3)_c$. The influence of the potential can be characterized by the two dimensionless parameters s and $x=\beta E_R$. Since we are only considering small values of the potential amplitude s, we find the thermodynamic quantities to quadratically depend on s to a very good degree of approximation (as long as the other parameters $\hat{a}$ and x held fixed). A linear behavior can of course be ruled out since the results should be independent of the sign of s.

To characterize the effect of the periodic potential on the critical properties, we will therefore focus on their behavior with the parameter x. For $x\gg 1$, one might intuitively expect the system to be well described by an "effective-mass model" where the influence of the periodic potential is accounted for by replacing the bare mass in the z direction with the effective mass at $\kappa_3=0$. However, the renormalization of the potential amplitude leads to significant quantitative deviations from such a simple behavior. In the limit of $x\ll 1$, the periodic potential becomes a long-wavelength perturbation to which $(\beta\mu)_c$ and f_c react very differently. The critical chemical potential depends on perturbative short-distance physics and is thus hardly affected by the presence of the potential. The particle number, however, is determined by the long-distance properties of the system and thus depends very sensitively on both x and $\hat{a}$ since the latter sets the length scale for the nonperturbative long-wavelength effects.

In Sec. V A, we will describe the predictions of the effective-mass model. For completeness, the critical properties of the ideal gas are briefly discussed in Sec. V B. Sections V C and V D present the results from mean-field and renormalization-group theory, respectively, together with a discussion of the behavior of the critical properties.

A. Effective-mass model

For $x\gg 1$, the system effectively experiences only the bottom of the lowest energy band. We would thus expect an "effective-mass model" to be well applicable where we replace the bare mass m in the q_3 direction by the effective mass $m^*=\alpha m$ at the bottom of the band, but neglect the

periodic potential otherwise. Simple scaling arguments for the partition function show that thermodynamically, this model is equivalent to a system with isotropic mass m, and modified mean particle density $n'=n/\sqrt{\alpha}$ and scattering length $\hat{a}'=\sqrt{\alpha}\hat{a}$ (we recall that $\hat{a}=a/\lambda_T$ in unscaled variables). Through this equivalence we can immediately derive the critical chemical potential and particle density in the effective-mass model. For the isotropic model, the particle density is given by [2]

$$n'\lambda_T^3=\zeta(3/2)+b_1\hat{a}'+O(\hat{a}'^2).$$

For the effective-mass model, we thus obtain

$$\begin{aligned} f_c &= \sqrt{\alpha}\zeta(3/2)+\alpha b_1\hat{a}+O(\hat{a}^2) \\ &\simeq \left(1+\frac{s^2}{16}\right)\zeta(3/2)+b_1\left(1+\frac{s^2}{8}\right)\hat{a}, \end{aligned} \tag{53}$$

where we have used the fact that $\alpha=1/(1-s^2/8)$ [see Eq. (8)]. In a similar way, one obtains

$$\begin{aligned} (\beta\mu)_c &= x\varepsilon^{(s)}(0)+4\zeta(3/2)\sqrt{\alpha}\hat{a}+O(\hat{a}^2) \\ &\simeq x\varepsilon^{(s)}(0)+4\zeta(3/2)\left(1+\frac{s^2}{16}\right)\hat{a}, \end{aligned} \tag{54}$$

where the term $x\varepsilon^{(s)}(0)$ is due to the ground-state energy. In Secs. V C and V D, we will see that the renormalization of the potential leads to significant corrections to the predictions of the effective-mass model.

B. Ideal gas

The scaled critical particle number $f_c^{(\mathrm{id})}$ of the ideal gas is given by Eq. (15). As discussed at the beginning of this section, the dependence of $f_c^{(\mathrm{id})}$ on the parameters s and x can be expressed as

$$f_c^{(\mathrm{id})}(s,x)=\zeta(3/2)[1+\bar{f}^{(\mathrm{id})}(x)s^2+O(s^4)], \tag{55}$$

where the essential effects of the periodic potential are summarized in the function $\bar{f}^{(\mathrm{id})}(x)$. In Fig. 1, this function is shown together with the approximations derived from Eqs. (16) and (17) At large x, $\bar{f}^{(\mathrm{id})}(x)$ follows the behavior expected from the effective-mass model. For decreasing x, $\bar{f}^{(\mathrm{id})}(x)$ goes through a maximum around $x\approx 3$ and then rapidly falls off to zero as soon as x becomes less than 1. As we will see, this behavior at small x is very different from the interacting case and illustrates that the condensation of the ideal gas is not sensitive to long-wavelength perturbations. We also note that $\bar{f}^{(\mathrm{id})}$ is always positive [except at very small x, where corrections to Eq. (17) need to be taken into account [20]]. This fact indicates that the shift in the number density is mostly determined by the low-energy regime [corresponding to $\varepsilon<1$ in Eq. (13)] where the density of states is increased as compared to the homogeneous gas. This behavior of $\bar{f}^{(\mathrm{id})}$ depends on the transverse confinement: for a harmonic potential the corresponding $\bar{f}^{(\mathrm{id})}$ becomes negative for $x<1$ [20,21] since the reduction in the density of states at higher energies becomes more relevant.

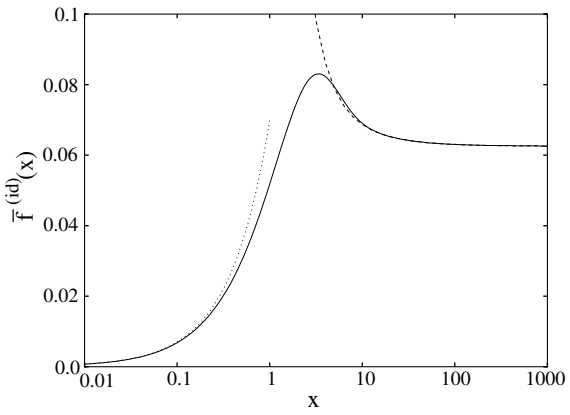

FIG. 1. Function $\bar{f}^{(\mathrm{id})}(x)$ characterizing the shift in the critical particle number for the ideal Bose gas, together with the approximations obtained from Eqs. (16) (dashed) and (17) (dotted). The asymptotic expansion (16) was calculated up to order x^{-3}.

C. Mean-field theory

As discussed in Sec. III, in the mean-field approach the critical thermodynamic quantities are obtained by solving Eq. (26) for s_{eff} with $\Delta\nu$ given by Eq. (29) at the phase transition. The critical chemical potential $(\beta\mu)_c$ is then determined from Eq. (27), whereas the particle number is given by $f_c=x\nu_0/2\hat{a}$. To identify the effects of the periodic potential on the critical chemical potential most clearly, we separate $(\beta\mu)_c$ into different contributions according to

$$\begin{aligned} (\beta\mu)_c &= x\varepsilon^{(s)}(0)+\Delta(\beta\mu)_c^{(\mathrm{MF})}(\hat{a},s=0)+4\zeta(3/2)\bar{v}^{(\mathrm{MF})}(x)s^2\hat{a} \\ &= x\varepsilon^{(s)}(0)+4\zeta(3/2)[1+\bar{v}^{(\mathrm{MF})}(x)s^2]\hat{a}. \end{aligned} \tag{56}$$

In this expression, $x\varepsilon^{(s)}(0)$ refers to the ground-state energy of the potential with *unrenormalized* amplitude s, which determines the critical chemical potential for the *ideal* Bose gas [note that, in contrast, Eq. (27) contains the renormalized quantity $x\varepsilon^{(s_{\mathrm{eff}})}(0)$]. The term $\Delta(\beta\mu)_c^{(\mathrm{MF})}(\hat{a},s=0)=4\zeta(3/2)\hat{a}$ describes the mean-field shift for the interacting *homogeneous* Bose gas. The additional interaction-induced shift in $(\beta\mu)_c$ caused by the presence of the periodic potential is given by the term $4\zeta(3/2)\bar{v}^{(\mathrm{MF})}(x)s^2\hat{a}$. The essential behavior of the shift, i.e., its variation upon a change of x, is thus described by the function $\bar{v}^{(\mathrm{MF})}(x)$.

Figure 2 shows the result of the numerical calculation of $\bar{v}^{(\mathrm{MF})}(x)$. The curves were obtained by evaluating $(\beta\mu)_c$ for fixed $\hat{a}$ and s as a function of x and extracting $\bar{v}^{(\mathrm{MF})}(x)$ according to Eq. (56). By subsequently varying s, the quadratic dependence of the shift on s as indicated in Eq. (56) was verified to a very good degree of approximation (this also applies to all other shift functions discussed in Secs. V C and V D). The bold curve displays $\bar{v}^{(\mathrm{MF})}(x)$ evaluated at $\hat{a}=10^{-5}$, whereas for the dotted curve $\hat{a}=10^{-2}$. The close agreement between these two curves shows that the residual dependence of $\bar{v}^{(\mathrm{MF})}(x)$ on $\hat{a}$ is rather weak.

The dash-dotted curve in Fig. 2 depicts the calculation of $(\beta\mu)_c$ with the renormalization of s not taken into account. In this case, $(\beta\mu)_c$ is given by Eqs. (27) and (28) with s_{eff} replaced by s. The critical particle density then equals the

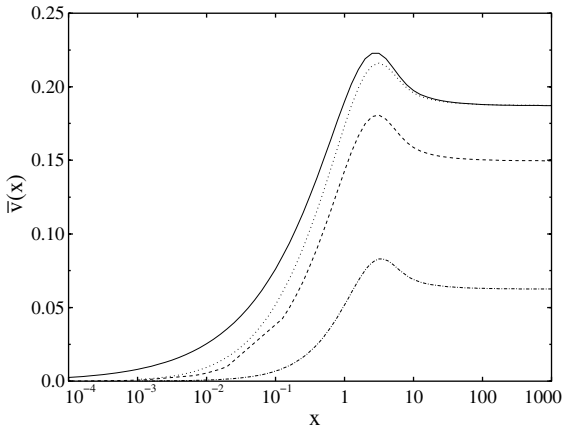

FIG. 2. Function $\bar{v}(x)$ characterizing the shift in the critical chemical potential for the interacting Bose gas. Full curve: $\bar{v}(x)$ for $\hat{a}=10^{-5}$ where MF and RG results coincide. Dashed (dotted) curve: $\bar{v}(x)$ for $\hat{a}=10^{-2}$ calculated with the RG (MF) approach. If potential renormalization is not taken into account, $\bar{v}(x)$ becomes equal to $\bar{f}^{(\mathrm{id})}(x)$ (dash-dotted curve).

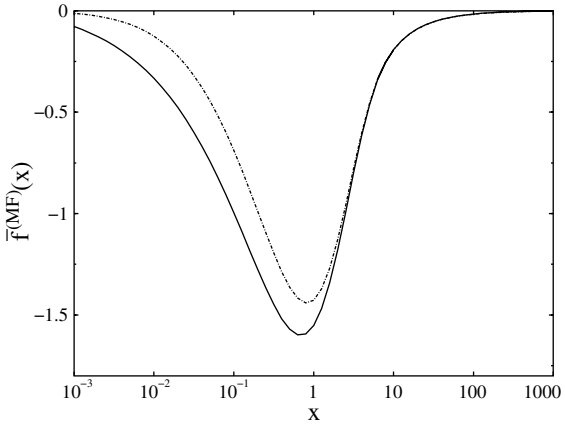

FIG. 3. Function $\bar{f}^{(\mathrm{MF})}(x)$ describing the shift in the critical density for the interacting Bose gas in the mean-field approximation. Full (dash-dotted) curve: $\bar{f}^{(\mathrm{MF})}(x)$ for $\hat{a}=10^{-5}$ ($\hat{a}=10^{-2}$).

one for the ideal gas with the same potential amplitude s, which implies that $\bar{v}^{(\mathrm{MF})}(x)$ is given by $\bar{f}^{(\mathrm{id})}(x)$ of Eq. (55). The large discrepancy between this calculation and the full result illustrates the significance of renormalization. In particular, we see that the calculation without renormalization agrees with the prediction of the effective-mass model in the limit of $x \gg 1$ since $\bar{v}$ tends against 0.0625 in this case. In the full calculation, however, a value of 0.1875 is attained. This result can be explained as follows. The critical chemical potential is given by Eq. (27). Using Eq. (29) one finds that $s_{\mathrm{eff}} \approx s[1-2\zeta(3/2)\hat{a}/x]$ for $x \gg 1$. The second term in Eq. (27) is hardly affected by the potential renormalization, i.e., $2x\nu_0 \approx 4\zeta(3/2)\hat{a}(1+s^2/16)$, which reproduces the result from the effective-mass model. To calculate the first term, we use $\varepsilon^{(s_{\mathrm{eff}})}(0) \approx -s_{\mathrm{eff}}^2/8$ so that $x\varepsilon^{(s_{\mathrm{eff}})}(0) \approx x\varepsilon^{(s)}(0)+4\zeta(3/2)\hat{a}s^2/8$. The mean-field induced shift in the effective ground-state energy thus leads to the additional contribution of 0.125 to the function $\bar{v}^{(\mathrm{MF})}(x)$.

It is also instructive to study the mean-field prediction for the critical particle number, although MF theory does not describe this quantity correctly. In the spirit of Eq. (56) we set

$$f_c = f_c^{(\mathrm{id})}(s,x) + \Delta f_c^{(\mathrm{MF})}(\hat{a},s=0) + \bar{f}^{(\mathrm{MF})}(x)s^2\hat{a} \qquad (57)$$

so that the function $\bar{f}^{(\mathrm{MF})}(x)$ again contains all relevant information on the shift in f_c caused by the periodic potential in the presence of interactions. The shift $f_c^{(\mathrm{id})}(s,x)$ for the ideal gas is given by Eq. (55). The mean-field shift in f_c for a homogeneous interacting gas vanishes, i.e., $\Delta f_c^{(\mathrm{MF})}(\hat{a},s=0)=0$ [1].

It follows from Eq. (28) that the mean-field critical particle density equals the critical density of an *ideal* gas in a periodic potential with amplitude s_{eff}. Thus, if we disregarded the potential renormalization (i.e., set $s_{\mathrm{eff}}=s$), there would be no additional shift $\bar{f}^{(\mathrm{MF})}(x)$ in mean-field theory. However, since $s_{\mathrm{eff}} \neq s$, we obtain a nonvanishing shift in contrast to MF theory for the homogeneous Bose gas. It should be noted that although this shift is linear in $\hat{a}$ as in the exact theory for the homogeneous Bose gas [2], the physical origins of the two shifts are completely different.

Figure 3 shows the numerical calculation of $\bar{f}^{(\mathrm{MF})}(x)$ for $\hat{a}=10^{-5}$ (full curve) and $\hat{a}=10^{-2}$ (dotted). Several aspects of these results should be noted. (i) As in the calculation of $\bar{v}(x)$, the shift $\bar{f}^{(\mathrm{MF})}(x)$ only displays a small residual dependence on $\hat{a}$. (ii) The function $\bar{f}^{(\mathrm{MF})}(x)$ is centered around $x=1$ with a "width" of about 2 in $\log_{10} x$ and goes to zero for $x \ll 1$ and $x \gg 1$. (iii) The fact that $\bar{f}^{(\mathrm{MF})}(x) \to 0$ for $x \gg 1$ is not in contradiction with the prediction (53) of the effective-mass model since the coefficient b_1 equals 0 in mean-field theory.

The subsequent RG calculation of f_c will yield qualitatively different behavior regarding the points (i) and (ii), thus emphasizing the inadequacy of the mean-field theory and the significance of nonperturbative effects.

D. RG theory

As described in Sec. IV, in the RG calculation of the critical thermodynamic quantities we have to determine the critical trajectories of the flow equations (48)–(50). From the initial conditions of these trajectories, we immediately obtain the critical chemical potential $(\beta\mu)_c$, whereas the critical particle density f_c is calculated from the derivative of the free energy as shown in Eq. (52). Similar to the calculations for mean-field theory, we distinguish different contributions to $(\beta\mu)_c$ and f_c according to

$$(\beta\mu)_c = x\varepsilon^{(s)}(0) + \Delta(\beta\mu)_c^{(\mathrm{RG})}(\hat{a},s=0) + 4\zeta(3/2)\bar{v}^{(\mathrm{RG})}(x)s^2\hat{a}, \qquad (58)$$

$$f_c = f_c^{(\mathrm{id})}(s,x) + \Delta f_c^{(\mathrm{RG})}(\hat{a},s=0) + \bar{f}^{(\mathrm{RG})}(x)s^2\hat{a}. \qquad (59)$$

Here, $\Delta(\beta\mu)_c^{(\mathrm{RG})}$ and $\Delta f_c^{(\mathrm{RG})}$ denote the interaction-induced shifts for the homogeneous Bose gas as determined by the

RG calculation. In contrast to MF theory, these quantities are not given by simple expressions, but have to be determined numerically, in general [18]. The functions $\bar{v}^{(\mathrm{RG})}(x)$ and $\bar{f}^{(\mathrm{RG})}(x)$ again characterize the additional shifts caused by the periodic potential in the presence of particle interactions.

In Fig. 2, $\bar{v}^{(\mathrm{RG})}(x)$ is depicted for $\hat{a}=10^{-5}$ (full curve) and $\hat{a}=10^{-2}$ (dashed). For $\hat{a}=10^{-5}$, the RG calculation is indistinguishable from MF theory. This illustrates the fact that, at least to leading order in the scattering length, the critical chemical potential is not influenced by long-wavelength critical fluctuations so that mean-field theory becomes applicable. In this context, we also note that $\bar{v}(x)$ becomes very small for $x \lesssim 10^{-3}$. This is another illustration of the fact that long-wavelength perturbations do not affect the critical chemical potential. For the larger value of $\hat{a}=10^{-2}$, some deviations between the RG and MF results appear. They are caused by higher-order contributions to $(\beta\mu)_c$ in the scattering length which are accounted for by the RG calculation but are absent in MF. However, these deviations are not very pronounced and affect neither the general shape nor the location of the shift function $\bar{v}(x)$. If we do not take the renormalization of the potential into account, i.e., if we set $s(l)=s(0)$ in Eqs. (48) and (49), then for small $\hat{a}$ the function $\bar{v}^{(\mathrm{RG})}(x)$ again becomes equal to $f^{(\mathrm{id})}(x)$ as in mean-field theory (for larger $\hat{a}$, slight deviations occur due to higher-order contributions in $\hat{a}$, which are absent in the MF calculation).

It is straightforward to relate the effective-mass model of Sec. V A to the present RG formalism. Starting from an effective action corresponding to the effective-mass model (i.e., a homogeneous system with an anisotropic mass tensor where one of the masses has been changed to αm), one obtains a system of flow equations (48), (49), and (51) with $\xi(l)$ replaced by $\sqrt{\alpha}$. It is then easy to see that these flow equations lead to the same conclusions regarding the critical particle number and chemical potential as expressed by Eqs. (53) and (54). In other words, the effective-mass model corresponds to a situation where we neglect the renormalization of the potential and consider the regime of $x \gg 1$, where $\xi(l) \approx \sqrt{\alpha}$ already at the beginning of the integration of the flow equations [in general, $\xi(l)$ will tend to $\sqrt{\alpha}$ only in the limit $l \to \infty$ as αm characterizes the effective mass at the *bottom* of the lowest energy band].

These considerations will be useful for the discussion of the critical particle density in the RG approach. To interpret the behavior of the shift function $\bar{f}^{(\mathrm{RG})}(x)$, it is helpful to first consider the situation in which the renormalization of the potential is *not* taken into account. Corresponding results for $\bar{f}^{(\mathrm{RG})}(x)$ are shown in Fig. 4 for values of $\hat{a}$ between 10^{-5} and 10^{-2}. We see that the behavior of the curves differs in two essential ways from the shift functions examined before. (i) The shift approaches zero, i.e., effects of the periodic potential become insignificant, only for much smaller values of x than encountered before. For example, for $\hat{a}=10^{-5}$, $\bar{f}^{(\mathrm{RG})}(x)$ becomes small only for $x \lesssim 10^{-9}$. (ii) The functions $\bar{f}^{(\mathrm{RG})}(x)$ now display a very pronounced characteristic dependence on the interaction strength $\hat{a}$. It manifests itself as a shift of the transition regime, which is apparent in the behavior of $\bar{f}^{(\mathrm{RG})} \times(x)$, toward larger x for growing $\hat{a}$.

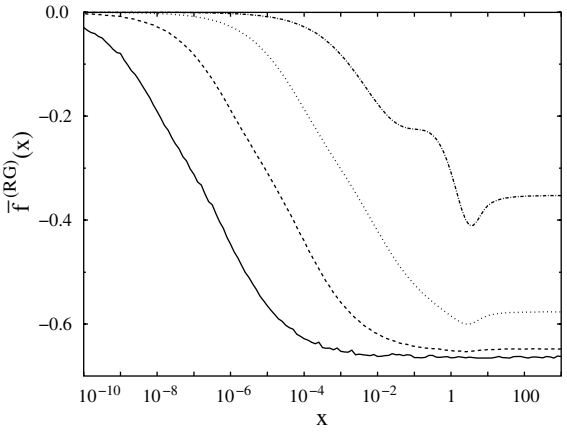

FIG. 4. Function $\bar{f}^{(\mathrm{RG})}(x)$ describing the critical-density shift in the RG calculation *without* renormalization of the potential amplitude. The curves show $\bar{f}^{(\mathrm{RG})}(x)$ for $\hat{a}=10^{-5}$ (full), 10^{-4} (dashed), 10^{-3} (dotted), and 10^{-2} (dash-dotted).

How can this behavior be explained? To this end, we recall that the homogeneous interacting Bose gas at criticality is characterized by an important microscopic momentum scale k_c [2,7,19]. This scale divides the regimes of perturbative short-distance and nonperturbative long-distance physics. In the single-particle dispersion relation $E(k)$ of the interacting critical Bose gas, it separates the region of large momenta where the spectrum is free-particle-like from the small-momentum region where the spectrum "hardens" and behaves like $k^{2-\eta}$ with η the anomalous dimension. The hardening of the spectrum is caused by the interaction-induced correlations between the atoms with momenta $k \lesssim k_c$ and leads to the shift in the critical particle number with growing interaction strength. The characteristic momentum k_c has been predicted to be proportional to $a/\tilde{\lambda}_T^2$ (with unscaled a and $\tilde{\lambda}_T=\lambda_T/k_l$).

The presence of a weak periodic potential now introduces another independent momentum scale given by k_l. It is now reasonable to assume that for $k_l \ll k_c$, the external potential should have no influence on the critical particle correlations due to its extremely long spatial period. There should thus be no additional shift in the critical particle density due to the periodic potential. On the other hand, for $k_l \gg k_c$ the critical long-wavelength fluctuations only sample a very small region in the center of the first Brillouin zone. We thus expect a situation like that in the effective-mass model: the total interaction-induced shift of the critical particle number should be the same as for a homogeneous Bose gas with an anisotropic mass tensor determined by the effective mass at the bottom of the lowest energy band.

The results of Fig. 4 confirm this expectation. For $x \ll 1$, i.e., very small k_l, the shift function $\bar{f}^{(\mathrm{RG})}(x)$ goes to zero, whereas for sufficiently large x it assumes the value expected for the effective-mass model. To see the latter, we recall that Eq. (53) predicts $\bar{f}^{(\mathrm{RG})}(x)=b_1/8$, where $b_1=-5.3$ in the RG theory [18]. For small $\hat{a}$, $\bar{f}^{(\mathrm{RG})}(x)$ indeed tends toward $-0.66 \approx -5.3/8$; for larger $\hat{a}$, higher-order corrections to Eq. (53) have to be taken into account. The most convincing

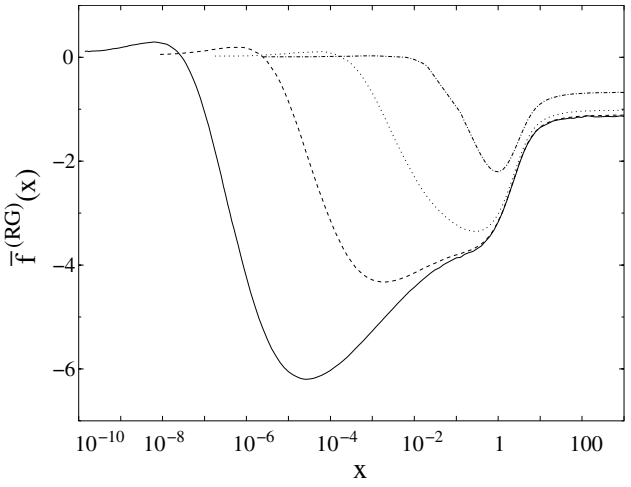

FIG. 5. Function $\bar{f}^{(\mathrm{RG})}(x)$ characterizing the shift in the critical particle density due to the periodic potential in the presence of interactions. The curves show $\bar{f}^{(\mathrm{RG})}(x)$ for $\hat{a}=10^{-5}$ (full), 10^{-4} (dashed), 10^{-3} (dotted), and 10^{-2} (dash-dotted), and are calculated following the RG approach of Sec. IV.

argument supporting the above interpretation, however, comes from the behavior of the transition region between these two limiting regimes. Since $k_c \sim a/\tilde{\lambda}_T^2$ and $x \sim k_l^2$, we can expect the location of the transition region along the x axis in Fig. 4 to scale with $\hat{a}^2$. The calculated curves indeed obey this behavior very accurately. Furthermore, the center of the transition region can roughly be characterized by $k_c \approx k_l$. Setting $k_c = Ca/\tilde{\lambda}_T^2$, one finds this condition to correspond to a "critical value" of x given by $x_c \approx C^2\hat{a}^2/4\pi$. Determining x_c from the point where $\bar{f}^{(\mathrm{RG})}(x)$ has dropped to half its value at $x \to \infty$, we find $C \approx 135$. Given the fact that k_c is not sharply defined but rather characterizes a crossover regime, this value is in reasonable agreement with the estimate $C \approx 20.7$ of Ref. [19]. Altogether, the observations described above strongly support the interpretation of Fig. 4 in terms of an interplay between the two independent momentum scales k_c and k_l.

Figure 5 shows the calculation of $\bar{f}^{(\mathrm{RG})}(x)$ including the renormalization of the potential. We see that the main qualitative features apparent in Fig. 4 still persist; however, the potential renormalization leads to strong quantitative modifications. In particular, the following aspects should be mentioned. (i) For $x \to \infty$, i.e., in the "effective-mass" regime, $\bar{f}^{(\mathrm{RG})}(x)$ still tends toward a constant value. For small $\hat{a}$, the effects of potential renormalization increase this value by more than 70% from what is expected from the effective-mass model. (ii) The deviations from the asymptotic constant behavior start at much larger x than in Fig. 4 and do not strongly vary with $\hat{a}$, initially. This behavior might be connected to the contribution to the shift, which is already present in mean-field theory (see Fig. 3) and which becomes relevant around similar values of x. (iii) At sufficiently small x, the scaling behavior of the transition region with a^2 that was discussed above is still clearly visible. (iv) For $x \to 0$, the shift function $\bar{f}^{(\mathrm{RG})}(x)$ goes to zero, but at a larger value of x than before. (v) Overall, the absolute values of $\bar{f}^{(\mathrm{RG})}(x)$ are much larger than in Figs. 3 and 4. It should thus be possible to experimentally observe the effects of the periodic potential on the critical particle number even for relative small values of s where the present theory is safely applicable.

VI. SUMMARY AND CONCLUSIONS

This paper presents a study of the phase transition of an interacting Bose gas in a weak periodic potential. Our theoretical approach relies on a description of the interplay between the effects of interactions and the external potential in terms of a renormalization of the potential amplitude. On this basis, we first develop a mean-field theory in order to qualitatively understand the significance and consequences of the potential renormalization. Quantitatively, MF theory allows us to describe properties of the phase transition depending on short-distance perturbative physics such as the behavior of the critical chemical potential. However, since the periodic potential does not reduce the influence of long-wavelength critical fluctuations, we need to go beyond MF theory to obtain a more complete understanding of the phase transition and, in particular, the behavior of the critical particle density. To this end, we have developed an RG approach which is based on the work of Refs. [10,17,18] but is extended in several ways to account for the presence of the periodic potential. The agreement between MF and RG theory regarding the calculation of the critical chemical potential indicates the consistency of the two approaches. Further evidence for the reliability of the RG approach is gained from studying the behavior of the critical particle density.

A main result of our investigation is the observation that with the help of a periodic potential, the existence of the characteristic nonperturbative momentum scale k_c can be made macroscopically manifest in the thermodynamic properties of the system. Depending on whether the wave vector k_l of the potential is larger or smaller than k_c, the behavior of the critical particle will or will not be sensitive to the presence of the periodic potential. Furthermore, our studies illustrate the significant effect that the renormalization of the potential has on the quantitative description of the thermodynamic properties; in particular, they demonstrate that in the short-wavelength limit for the periodic potential, a simple effective-mass model does not provide an adequate and correct description.

Interaction-induced shifts in the critical temperature have already been observed in harmonically trapped Bose gases [37]. Corresponding experiments with homogeneous Bose gases, although significantly more difficult, thus should also be feasible as soon as technical problems regarding, e.g., the construction and loading of suitable traps or the measurement of the temperature have been solved. Once such experiments are possible, it should not be too difficult to also test some of the main predictions of this work. The periodic potential can be realized with the help of optical standing waves. By varying the wavelength of the periodic potential and the condensation temperature, it should be feasible to change the parameter x over several orders of magnitude (note that x is proportional to the inverse square of the wave-

length). By tuning the intensity of the laser fields generating the standing waves, the amplitude parameter s can be varied almost arbitrarily.

It is difficult to estimate accurately up to what values of s the present approach is valid. However, some indication can be obtained from the ideal gas if one compares the shift in the critical temperature obtained from our main approximation (6) and shown in Fig. 1 to the result calculated from the exact dispersion relation for the gas in the potential (1). Such a comparison suggests that the approximation (6) can safely be applied for values of s up to 1. Of course, in the interacting case further approximations are involved, but we do not expect them to significantly reduce the limits on s. For values of s of the order of 1, we can already expect the periodic potential to give rise to significant corrections to the critical properties of the interacting gas. We also emphasize that applying the periodic potential in all three spatial directions should significantly enhance the effects described in this paper without changing them qualitatively. We expect that it should be possible to extend the present formalism to this case without major modifications.

An immediate extension of the present work would be the study of condensation in a harmonic trap with a superimposed weak periodic potential. Assuming the harmonic trap to be sufficiently wide, we can invoke the local-density approximation. We can then use it together with the mean-field or the RG description, as they have been developed here for the gas with a homogeneous background, to study the thermodynamic properties and the critical behavior of the trapped system.

[1] J. O. Andersen, Rev. Mod. Phys. **76**, 599 (2004).
[2] G. Baym, J.-P. Blaizot, M. Holzmann, F. Laloë, and D. Vautherin, Phys. Rev. Lett. **83**, 1703 (1999).
[3] M. Holzmann, G. Baym, J.-P. Blaizot, and F. Laloë, Phys. Rev. Lett. **87**, 120403 (2001).
[4] P. Arnold and G. Moore, Phys. Rev. Lett. **87**, 120401 (2001).
[5] P. Arnold and G. D. Moore, Phys. Rev. E **64**, 066113 (2001).
[6] V. A. Kashurnikov, N. V. Prokof'ev, and B. V. Svistunov, Phys. Rev. Lett. **87**, 120402 (2001).
[7] P. Arnold, G. Moore, and B. Tomásik, Phys. Rev. A **65**, 013606 (2002).
[8] S. Giorgini, L. P. Pitaevskii, and S. Stringari, Phys. Rev. A **54**, R4633 (1996).
[9] P. Arnold and B. Tomásik, Phys. Rev. A **64**, 053609 (2001).
[10] O. Zobay, G. Metikas, and G. Alber, Phys. Rev. A **69**, 063615 (2004).
[11] O. Zobay, J. Phys. B **37**, 2593 (2004).
[12] O. Zobay, G. Metikas, and H. Kleinert, Phys. Rev. A **71**, 043614 (2005).
[13] W. Zwerger, J. Opt. B: Quantum Semiclassical Opt. **5**, S9 (2003).
[14] H. Kleinert, S. Schmidt, and A. Pelster, Phys. Rev. Lett. **93**, 160402 (2004).
[15] R. Ramakumar and A. N. Das, Phys. Rev. B **72**, 094301 (2005).
[16] B. G. Wild, P. B. Blakie, and D. A. W. Hutchinson, Phys. Rev. A **73**, 023604 (2006).
[17] G. Metikas, O. Zobay, and G. Alber, Phys. Rev. A **69**, 043614 (2004).
[18] O. Zobay, Phys. Rev. A **73**, 023616 (2006).
[19] G. Baym, J.-P. Blaizot, M. Holzmann, F. Laloë, and D. Vautherin, Eur. Phys. J. B **24**, 107 (2001).
[20] M. Rosenkranz and O. Zobay (unpublished).
[21] M. Rosenkranz, Diploma thesis, Technical University Darmstadt (2006).
[22] A. L. Fetter and J. D. Walecka, *Quantum Theory of Many-Particle Systems* (McGraw-Hill, New York, 1971).
[23] M. Holzmann, J. N. Fuchs, G. Baym, J. P. Blaizot, and F. Laloë, C. R. Phys. **5**, 21 (2004).
[24] M. Haque, e-print cond-mat/0302076 (2003).
[25] G. Metikas, O. Zobay, and G. Alber, J. Phys. B **36**, 4595 (2003).
[26] K. Berg-Sørensen and K. Mølmer, Phys. Rev. A **58**, 1480 (1998).
[27] K.-P. Marzlin and W. Zhang, Phys. Rev. A **59**, 2982 (1999).
[28] D.-I. Choi and Q. Niu, Phys. Rev. Lett. **82**, 2022 (1999).
[29] K. G. Wilson and J. Kogut, Phys. Rep., Phys. Lett. **12**, 75 (1974).
[30] K. K. Singh, Phys. Rev. B **12**, 2819 (1975).
[31] R. J. Creswick and F. W. Wiegel, Phys. Rev. A **28**, 1579 (1983).
[32] D. S. Fisher and P. C. Hohenberg, Phys. Rev. B **37**, 4936 (1988).
[33] M. Bijlsma and H. T. C. Stoof, Phys. Rev. A **54**, 5085 (1996).
[34] J. O. Andersen and M. Strickland, Phys. Rev. A **60**, 1442 (1999).
[35] G. Alber, Phys. Rev. A **63**, 023613 (2001).
[36] G. Metikas and G. Alber, J. Phys. B **35**, 4223 (2002).
[37] F. Gerbier, J. H. Thywissen, S. Richard, M. Hugbart, P. Bouyer, and A. Aspect, Phys. Rev. Lett. **92**, 030405 (2004).